IRAQI JOURNAL OF MATERIALS
Volume (3) Issue (1) January-March 2024, pp. 19-24

Plasma-Induced Growth of Silicon Carbide on Silicon Substrate for Heterojunction Fabrication

Oday A. Hammadi

Department of Physics, College of Education, Al-Iraqia University, Baghdad, IRAQ

Abstract
In this work, p-type silicon substrates were etched and coated with graphite paste to form layers of n-type silicon carbide by plasma-induced bonding technique. The structures and morphology of these structures were introduced by x-ray diffraction (XRD), scanning electron microscopy (SEM) and atomic force microscopy (AFM). These tests confirmed the formation of nanostructured SiC layers on the etched Si substrates. Electrical characteristics showed that the formed n-SiC/p-Si anisotype heterojunction has an ideality factor of 0.45 and the built-in potential was measured to be 2.6V. This technique is reasonably efficient, low-cost and reliable to fabricate heterojunctions from nanostructured compound semiconductors on silicon substrates.

Keywords: Heterojunction; Plasma-induced bonding; Silicon carbide; Nanostructures
Received: 9 September 2023; **Revised:** 8 November; **Accepted:** 15 November; **Published:** 1 January 2024

1. Introduction

Recently, silicon carbide attracts a lot of interest by research works due to its intensive use in high-temperature, high-power and high-frequency applications. This compound semiconductor is increasingly replacing silicon in micro-electro-mechanical systems (MEMS) and nano-electro-mechanical systems (NEMS) operating in harsh environments, and too many devices used for automotive, petrochemical and aerospace applications [1-3]. This material is effectively used in non-oxide ceramic applications [4].

Silicon carbide is a polymorphic compound that can be found in 200 polytypes and crystallographic configurations [5]. It is a wide-band-gap semiconductor (2.3-3.2 eV). It has high breakdown electric field, high thermal conductivity, relatively high oxidation resistance, high chemical stability, high hardness, high melting point, high electron mobilities and low intrinsic carrier concentrations, which lead to stable electronic properties in harsh environments [1, 6-7].

Silicon carbide nanostructures are well known as highly-functionalized material and the quantum confinement effect causes the photoluminescence of SiC nanocrystals is shifted towards the blue region of spectrum [8-13]. Accordingly, SiC nanostructures are effectively used in nano-scale light emitters, nano-optoelectronics and biological and medical labels [14]. The luminescent properties of SiC nanocrystals depend on their fabrication method [15-17].

Amongst all SiC crystallographic configurations, the 3C- or □-SiC takes an exceptional importance in applications. It is fabricated by many and various methods and techniques, such as chemical vapor deposition (CVD), plasma-enhanced CVD (PECVD), electrochemical etching, reduction-carburization route (RCR), sol-gel, molecular beam epitaxy (MBE), physical vapor transport (PVT), magnetron sputtering, pulsed-laser ablation (PLA), liquid-phase sintering (LPS) and mechanical alloying (MA) [18-30].

The heterojunction fabricated from SiC and silicon is one of the most promising devices for the next-generation power electronics due to its low breakdown voltage (~4V) and high reverse leakage current density (~$5x10^{-4}$A/cm^2 at 1V) [31]. Some other important devices, such as heterojunction bipolar transistors (HBTs), photovoltaic solar cells, high-voltage and high-frequency micro-electronics, are also based on this heterojunction [32-35].

In this work, the plasma-induced growth of nanostructured SiC layer on a plasma-etched silicon substrate is employed to fabricate n-SiC/p-Si heterojunction photodetector. The structural and electrical characteristics of this heterojunction are introduced.

2. Experiment

A p-type (100) orientated silicon wafer with resistivity of 15–20 □.cm, diameter of 5cm and thickness of 650 µm was used as substrate. The wafer was cleaned using 5% HF solution and acetone. Then, it was placed on a flat stainless steel disc with a diameter of 6cm and thickness of 5mm and then mounted by a similar stainless steel disc with a central window of 1cm diameter, as shown in Fig. (1), which was completely covered by the generated plasma column. This assembly represents the cathode of glow discharge system while the anode was a stainless steel assembly of the same dimensions. The deposition chamber was first evacuated to 10^{-6} mbar to remove any residual gases and contaminations in order to prevent the formation any silicon compounds (especially SiO_2) other than silicon carbide. Highly-pure (~99.9%) argon gas was used to generate the discharge plasma.

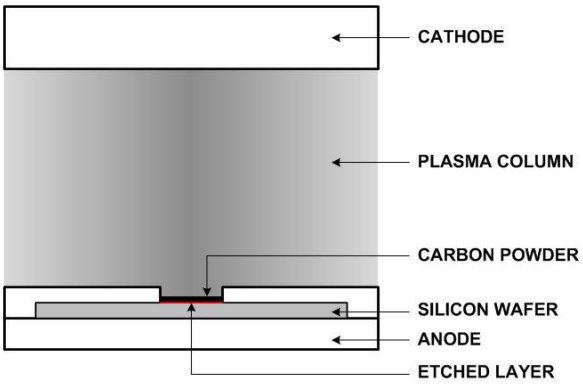

Fig. (1) The expwerimental arrangement used in this work

The silicon wafer was etched by plasma at gas pressure of 0.08 mbar, discharge voltage of 1.5 kV and discharge current of 20 mA for 30 minutes to form nanoscale rough surface (~4nm) over the area exposed to the plasma column. Similar work was previously performed by author [36]. The polarity of discharge electrodes was converted and the central window was then filled with a 100-200 µm thick layer of carbon (graphite paste of 25µm grain size) to reach the nano-scale rough surface of the silicon wafer. The sample was processed by plasma generated at gas pressure of 0.15 mbar, discharge voltage of 3.5 kV, discharge current of 45 mA for 5 hours. The sample was cleaned by HF and HCl to remove the graphite particles may reside after processing with plasma. The thickness of SiC layer was measured by ellipsometry method and found to be 90±5nm.

The sample holder could be heated by an external electrical heater to 800°C and a K-type thermocouple was used to measure the temperature on the surface of the anode during plasma processing.

The x-ray diffraction (XRD), scanning electron microscopy (SEM), atomic force microscopy (AFM) tests were performed to introduce the structural characteristics of the fabricated structures. As well, for photoluminescence (PL) measurements, a He-Cd laser beam with a wavelength of 325nm was used for the excitation and the photoluminescent light was dispersed using a double grating spectrometer with focal length of 500 mm and detected by a photomultiplier. With this setup the resolution in photon energy is better than 0.5 meV.

As well, the electrical characteristics of the fabricated heterojunction were determined using a dc voltage supply (0-300V) and picoammeter to measure the electrical current. An OSRAM 20W halogen lamp emitting in the UV region was used for illumination conditions of electrical characteristics. Aluminum contacts were deposited on the front and back sides of the fabricated sample to carry out the electrical measurements.

3. Results and Discussion

The XRD pattern of the fabricated sample shown in Fig. (2) confirmed the formation of polycrystalline structure and the five peaks apparently observed on this pattern at 2□ of 35.7°, 41.4°, 60.0°, 71.8° and 75.5° corresponding to lattice planes of (111), (200), (220), (310) and (222), respectively, are belonging to the □-SiC compound. These lattice planes confirm the formation of face-centered cubic (f.c.c.) SiC compound. However, there are two peaks observed at 2□ of 26.5° and 34°, which attributed to graphite residual in the sample after plasma processing. This result assign that the ratio of □-SiC in the final

product may reach to 90% as very little amount of graphite was observed and no pure silicon was observed.

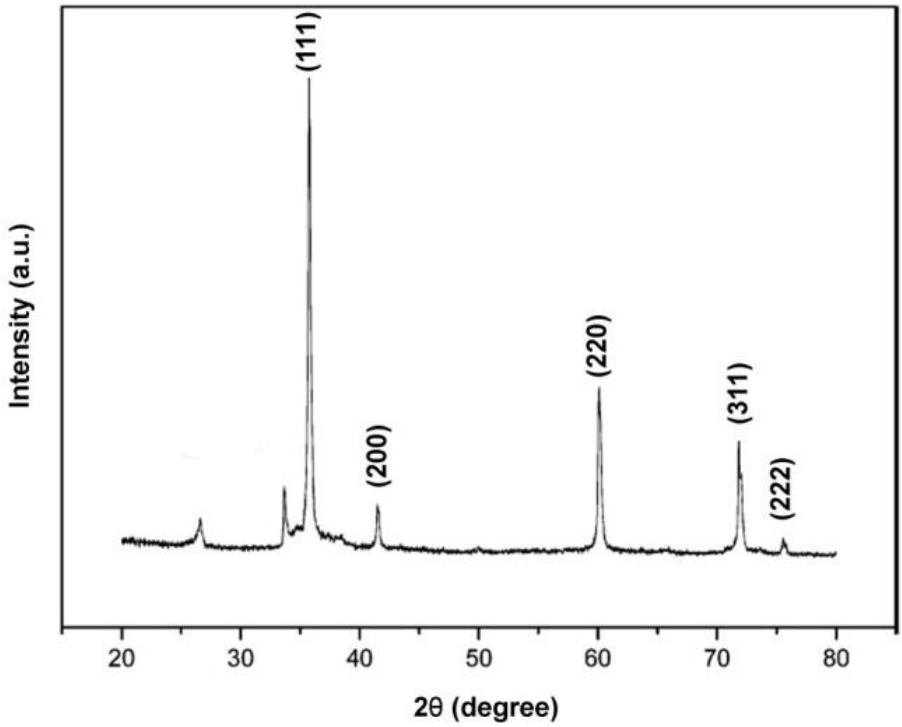

Fig. (2) XRD pattern of nanostructured SiC layer grown in this work

Figure (3a) shows the AFM topography of the plasma-etched silicon surface before covered with carbon powder. The root-mean-square roughness ($R_{r.m.s}$) of this surface was reasonably decreased, as shown in Fig. (3b), after the formation of silicon carbide layer, which was induced by plasma.

In order to confirm the formation of SiC nanoparticles, the final sample was characterized by SEM, as shown in Fig. (4), and an average particle size of 50nm was determined. Despite the high purity of the formed nanostructure observed from Fig. (4), very few agglomerations can be observed and attributed to the thermal effect of plasma processing, which is reasonably a random distribution of thermal energies over the volume of plasma column. The temperature at the processing area was measured to be 500°C.

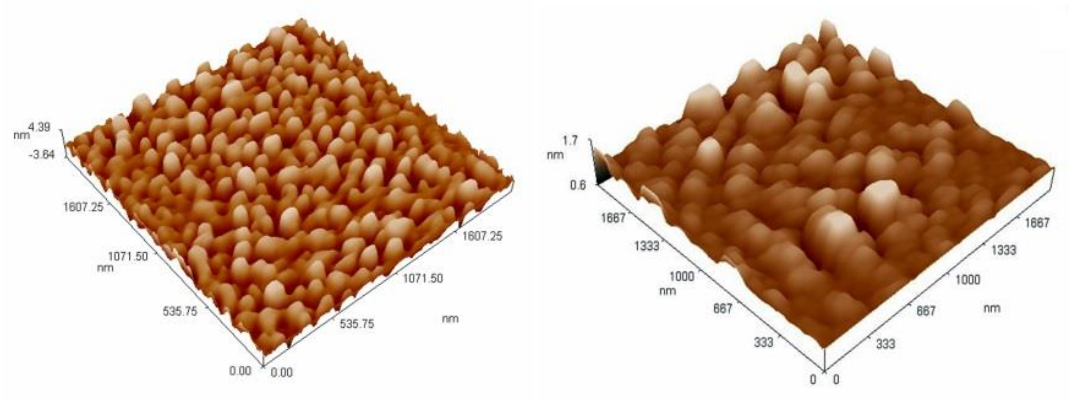

(a) **(b)**

Fig. (3) Topography of bare etched silicon layer (a) and grown SiC layer (b)

The photoluminescence (PL) spectrum of the fabricated SiC sample is shown in Fig. (5) and obtained at an excitation wavelength of 325nm. Visible PL has been observed from these systems, which opened up the possibility of the integration photonics with silicon-based microelectronics. The PL arising from

most of these materials is located in the red or yellow-green spectral region. There were two photoluminescence bands observed at 435 and 535nm corresponding to photon energies of 2.85 and 2.32 eV, respectively (energy band gap of SiC is ~2.4eV). Also, a blueshift of ~15nm was shown and attributed to the fact that the smaller particles of SiC may be a source for such shift as these particles are not easily oxidized at room temperature.

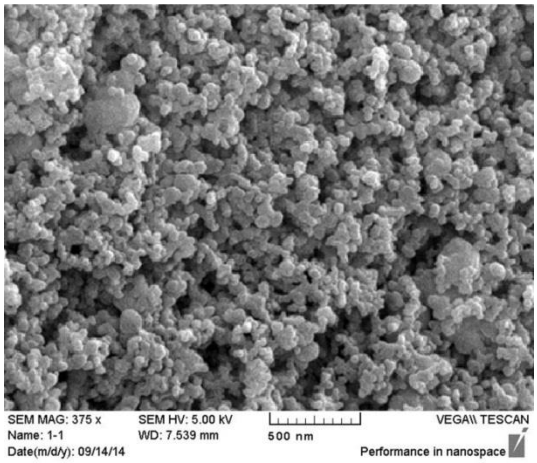

Fig. (4) SEM micrograph of the SiC layer grown in this work

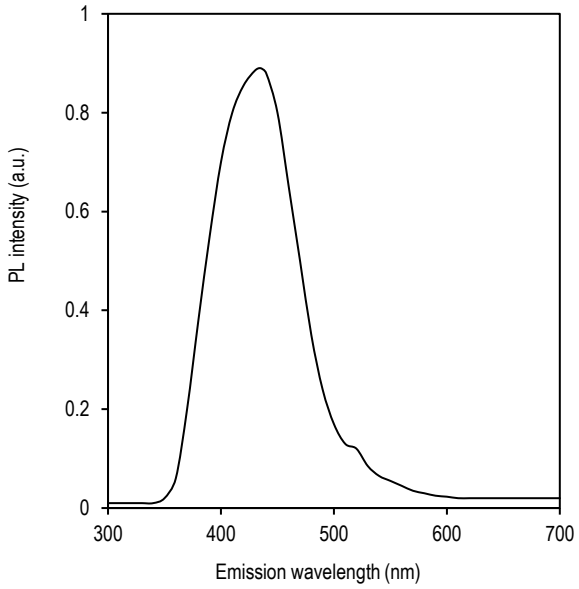

Fig. (5) PL spectrum of the SiC sample grown in this work

Figure (6) shows the current-voltage (I-V) characteristics of the fabricated n-SiC/p-Si heterojunction in both light and dark conditions. As shown, the dark current is about 30□A and the forward current is uniformly linear. The illumination current in the reverse biasing reaches a maximum of about 145□A. The bonded interface is often avoided in the electrically active region of the electronic device. However, the recombination centers of the defective bonded interface are used to control the minority carrier lifetime in power devices. Accordingly, the ideality factor of the fabricated junction can be determined to be 0.45 in the forward bias region and the deviation of ideality factor from the theoretical value (~1) is attributed to the assumption of the current transport explained by means of carrier recombination through multiple deep and shallow levels in the band gap of SiC.

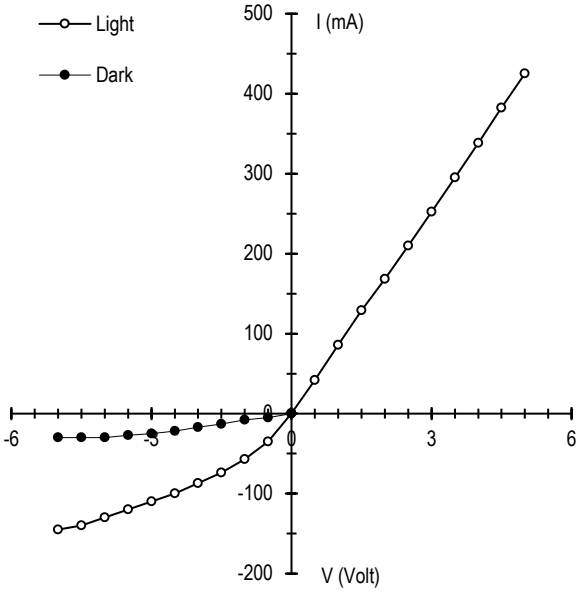

Fig. (6) The I-V characteristics in dark and light for the SiC-Si heterojunction fabricated in this work

In order to introduce the nature of the anisotype SiC/Si heterojunction, the C-V measurements were performed in the reverse biasing and results are presented in Fig. (7). The straight line of the curve confirmed that the junction is abrupt and the built-in potential was determined for the SiC/Si heterojunction to be about 2.6V.

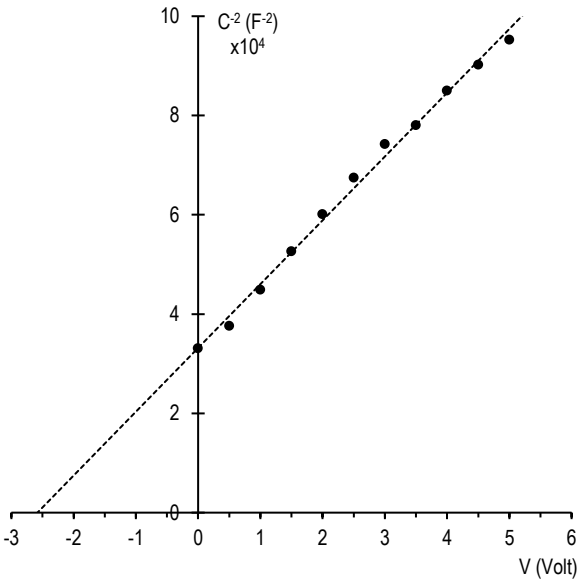

Fig. (7) The C-V characteristics of the SiC-Si heterojunction. The value of V_{bi} is about 2.6eV

4. Conclusion

According to the obtained results, an anisotype heterojunction was fabricated by the growth of a nanostructured layer of n-type silicon carbide on a p-type silicon wafer. The growth of this layer was induced by argon discharge plasma. The structural characteristics showed that the grown layer is □-SiC with an average particle size of 50nm. There were two photoluminescence bands observed at 435 and 535nm corresponding to photon energies of 2.85 and 2.32 eV, respectively. The electrical characteristics showed that the fabricated heterojunction has approximately linear behavior in the forward bias condition, the maximum dark current is about 145μA, the ideality factor is 0.45, the junction is abrupt

 ISSN (print) 2958-8960 (online) xxxx-xxxx Printed in IRAQ

and the built-in potential is about 2.6V. The technique employed in this work is reasonably efficient, low cost and reliable to fabricate heterojunctions for high-temperature electronic devices.

References

[1] O.A. Hamadi, K.Z. Yahiya and O.N.S. Jassim, *J. Semicond. Technol. Sci.*, 5(3), 69-73 (2005).
[2] P.M. Sarro, *Sensors and Actuators: Physical*, 82(1-3), 210-218 (2000).
[3] Y.T. Yang et al., *Appl. Phys. Lett.*, 78(2), 162-164 (2001).
[4] J.A. Di Carlo and H.-M. Yun, **Non-oxide (Silicon Carbide) Fibers, in Handbook of Ceramic Composites,** N.P. Bansal (ed.) (Springer, 2005), Ch. 2, pp. 33-52.
[5] I. V. Derevyanko and O. I. Polyakov, *Metall. Mining Indust.*, 4(4), 14-18 (2012).
[6] H.K. Seong et al., *Appl. Phys. Lett.*, 85(7), 1256-1258 (2004).
[7] O.A. Hamadi, *Iraqi J. Appl. Phys. Lett.*, 3(1), 23-26 (2010).
[8] R.A. Andrievski, *Rus. Chem. Rev.*, 78(9), 821-831 (2009).
[9] K. Chen et al., *Ceramics Inter.*, 39, 1957-1962 (2013).
[10] W. Han et al., *Chem. Phys. Lett.*, 265, 374-378 (1997).
[11] J. Khamsuwan et al., *Nucl. Instrum. Methods in Phys. Res. B*, 282, 88-91 (2012).
[12] H. Zhang et al., *Nanoscale Res. Lett.*, 5, 1264-1271 (2010).
[13] X.W. Du et al., *Mater. Sci. Eng. B*, 136, 72-77 (2007).
[14] J.-M. Bluet et al., **SiC as a Biocompatible Marker for Cell Labeling, in "Silicon Carbide Biotechnology"**, S. Saddow (ed.) (Elsevier Science, 2012) *Ch. 11,* 377-429.
[15] K. Nagarajan and S. Kumara Raman, *Bulg. J. Phys.*, 35, 53-57 (2008).
[16] G. Xi et al., *J. Phys. Chem. B*, 109, 13200-13204 (2005).
[17] J.Y. Fan, X.L. Wu and P.K. Chu, *Prog. Mater. Sci.*, 51, 983-1031 (2006).
[18] S. Madapura, A.J. Steckl and M. Loboda, *J. Electrochem. Soc.*, 146(3), 1197-1202 (1999).
[19] P.H. Yih, J.P. Li and A.J. Steckl, *IEEE Trans. Electron Devices*, 41(3), 281-287 (1994).
[20] A. Gupta, D. Paramnik, S. Varma and C. Jacob, *Bull. Mater. Sci.*, 27(5), 445–451 (2004).
[21] C. R. Stoldt et al., *Appl. Phys. Lett.*, 79(3), 347-349 (2001).
[22] Y.T. Kim et al., *J. Ceramic Process. Res.*, 6(4), 294-297 (2005).
[23] J.H. Boo, S.A. Ustin and W. Ho, *Thin Solid Films*, 324, 124-128 (1998).
[24] K. Volz et al., *Mater. Sci. Eng. A*, 289, 255-264 (2000).
[25] G.S. Sun et al., *J. Cryst. Growth*, 227–228, 811–815 (2001).
[26] G. Leal et al., *Mater. Res.*, 17(2), 472-476 (2014).
[27] S. Yang, W. Cai, H. Zeng and X. Xu, *J. Mater. Chem.*, 19, 7119-7123 (2009).
[28] O.A. Hammadi, M.K. Khalaf and F.J. Kadhim, *Proc. IMechE, Part L, J. Mater.: Design and Applications*, 2015, doi: 10.1177/1464420715601151.
[29] O.A. Hammadi, M.K. Khalaf and F.J. Kadhim, *Opt. Quantum Electron.*, 2015, doi: 10.1007/s11082-015-0247-6.
[30] O.A. Hammadi, M.K. Khalaf and F.J. Kadhim, *Proc. IMechE, Part N, J. Nanomater. Nanoeng. Nanosyst.*, 230(1), 32-36 (2016).
[31] P. Tanner, S. Dimitrijev and H.B. Harrison, Proc. IEEE Conf. on Optoelectronic and Microelectronic Materials and Devices, COMMAD 2008 (28 July- 1 August, 2008, Sydney, Australia), 41-43.
[32] O.A. Hamadi and K.Z. Yahiya, *Sharjah Univ. J. Pure Appl. Sci.*, 4(2), 1-11 (2007).
[33] O.A. Hamadi, *Proc. IMechE, Part L, J. Mater.: Design and Applications*, 222, 65-71 (2008).
[34] O.A. Hammadi, *Photonic Sensors*, 5(2), 152-158 (2015).
[35] O.A. Hamadi, *Iraqi J. Appl. Phys.*, 4(3), 34-37 (2008).
[36] A.K. Yousif and O.A. Hamadi, *Bulg. J. Phys.*, 35(3), 191-197 (2008).

